JOURNAL OF THERMOPHYSICS AND HEAT TRANSFER
Vol. 22, No. 2, April–June 2008

Technical Notes

TECHNICAL NOTES are short manuscripts describing new developments or important results of a preliminary nature. These Notes should not exceed 2500 words (where a figure or table counts as 200 words). Following informal review by the Editors, they may be published within a few months of the date of receipt. Style requirements are the same as for regular contributions (see inside back cover).

Turbulent Aeroheating on the Mars Science Laboratory Entry Vehicle

Michael D. Bynum*
North Carolina State University, Raleigh, North Carolina 27695-7910
Brian R. Hollis†
NASA Langley Research Center, Hampton, Virginia 23681
and
H. A. Hassan‡ and X. Xiao§
North Carolina State University, Raleigh, North Carolina 27695-7910

DOI: 10.2514/1.33281

Nomenclature

C	=	specific heat of model material
C_p	=	specific heat at constant pressure of test gas
D	=	model diameter
k	=	turbulent kinetic energy/mass
M	=	Mach number
P	=	pressure
q	=	heat flux
R	=	model radius
Re_D	=	Reynolds number based on diameter
St	=	Stanton number
T	=	temperature
t	=	time
u	=	velocity
x	=	distance along the surface
y	=	distance normal to the surface
α	=	thermal diffusivity
ΔH	=	total enthalpy relative to wall conditions
ϵ	=	dissipation rate of k
ρ	=	density
ζ	=	variance of vorticity, or enstrophy
ω	=	ϵ/k

Subscripts

m	=	surface material
w	=	wall
∞	=	freestream

Presented as Paper 4393 at the 39th AIAA Thermophysics Conference, Miami, Florida, 25–28 June 2007; received 5 July 2007; revision received 10 July 2007; accepted for publication 30 July 2007.

*Research Assistant, Mechanical and Aerospace Engineering. Student Member AIAA.
†Aerospace Engineer, Aerothermodynamics Branch. Senior Member AIAA.
‡Professor, Mechanical and Aerospace Engineering. Fellow AIAA.
§Research Assistant Professor, Mechanical and Aerospace Engineering; currently at Corvid Technologies, Mooresville, North Carolina 28117. Member AIAA.

I. Introduction

THE Mars Science Laboratory (MSL) entry vehicle heat shield is a 70-deg sphere cone [1]. The current MSL mission profile differs from other missions because the vehicle has a greater size, entering mass, ballistic coefficient, and angle of attack than any of the previous missions. To accomplish a precision landing, the vehicle will be required to fly a controlled lifting trajectory at an angle of attack of 16 deg that will result in a lift-to-drag (L/D) ratio of 0.24. As a result, boundary-layer transition is expected to occur well before peak heating on the trajectory. Therefore, the heat shield is being designed assuming the flow to be turbulent.

Because of the turbulent design requirement, an experimental program was conducted with the goal of defining computational safety margins for turbulent conditions through comparison with wind-tunnel data [1]. The data considered here span a range of Reynolds numbers for baseline comparisons in a nonreacting environment. The focus of the research will be on the tests that were carried out at the Arnold Engineering Development Center (AEDC) Tunnel 9, which is a hypersonic, nitrogen gas, blowdown facility with interchangeable nozzles [2]. The tests were carried out at Mach numbers of 10 and 8 over a unit Reynolds number range of 0.054×10^6–48.4×10^6/ft (0.177×10^6–158.8×10^6/m). The Mach 10 conditions resulted mostly in laminar and transitional flows, whereas the Mach 8 conditions resulted in laminar, transitional, and turbulent flows. As a result, the bulk of comparisons are made with the Mach 8 turbulent data.

All calculations presented used the Langley aerothermodynamics upwind relaxation algorithm (LAURA) code [3,4]. Three sets of distinct turbulence models were employed: the Cebeci–Smith (CS) algebraic model [5], the 1998 Wilcox k–ω turbulence model [6], and the k–ζ turbulence model of Hassan and Robinson [7].

II. Formulation of the Problem

A. Turbulence Models

Three turbulence models are used in this investigation. Algebraic models are computationally fast and stable and are accurate for attached flows. The Cebeci–Smith algebraic model was used in calculating the various test cases used in Hollis and Collier [1] and again used here for comparison with the two-equation turbulence models. The other two models are the 1998 Wilcox k–ω and the Hassan and Robinson k–ζ, both of which are two-equation models. The quantity k represents the turbulent kinetic energy per unit mass, $\omega = \epsilon/k$, where ϵ is the dissipation rate of k and ζ is the variance of vorticity or enstrophy.

There are a number of important differences between the k–ω and k–ζ models. Most of the differences are a result of the fact that the two length scale equations, that is, the ω and ζ equations, are completely different. The ω equation is purely empirical. On the other hand, in

the k–ζ model, both equations are derived from the exact compressible momentum equations, and the resulting equations are modeled term by term. The resulting set of equations are tensorially and dimensionally consistent, Galilean invariant, and coordinate system independent and, in principle, model all of the relevant physics of turbulent flows as long as the Morkovin's assumption is valid.

The Cebeci–Smith and the 1998 Wilcox k–ω models were coded in LAURA earlier. On the other hand, the k–ζ model was implemented in LAURA by the present authors.

B. Experimental Setup

A 6-in. diameter (0.1524 m) model of the MSL outer mold liner (OML-6) configuration was fabricated from heat treated 15-5 stainless steel. The test model was instrumented with 39 Medtherm^{TM} type-E coaxial (chromel–constantan) thermocouples. A schematic gauge layout is shown in Fig. 1; 33 of the 39 gauges were located on the forebody. The thermocouples were fitted into the model through predrilled holes and fixed with Loctite^{TM} adhesive. The sheet thickness of the model (and thermocouple length) were specified at a nominal value of approximately 0.5 in. to ensure that the heat conduction into the model did not violate the semi-infinite assumption over the length of the AEDC Tunnel 9 test time, which is of the order of 1 s or less.

C. Data Reduction

There were a couple of issues that came up when reducing the AEDC data: one pertains to the manner in which the heat transfer is calculated, whereas the other corresponds to the probe and surface thermal properties.

Thermocouple voltage data from the AEDC Tunnel 9 was converted to temperature using the NIST standard calibration formula for type-E thermocouples. The resulting probe temperature was assumed to be the surface temperature, and this temperature was used in solving the heat conduction equation [Eq. (1)] to estimate the wall heat flux q:

$$\frac{\partial T}{\partial t} = \alpha \frac{\partial^2 T}{\partial y^2}, \qquad \alpha = \left(\frac{\lambda}{\rho C}\right)_m \tag{1}$$

where T is the temperature, λ is the coefficient of thermal conductivity, α is the thermal diffusivity, ρ is the density, and C is the specific heat for which the subscript m designates the material.

The major difficulty in the aforementioned procedure is that the probe, the Loctite^{TM} adhesive, and the surface have different conductivities and are not in perfect contact. As a result, using a one-dimensional calculation for a given surface temperature may result in some inaccurate heat flux. In particular, using the temperature measured by the probe in conjunction with either the probe or surface thermal properties will result in incorrect heat flux. This, indeed, was the case [1].

A chromel probe was employed and the AEDC 15-5 steel was used to construct the model. Using available thermal diffusivity values for both of these substances in Eq. (1) resulted in the wrong heat transfer when compared with the laminar flow calculations. After many trials, which are detailed in Hollis and Collier [1], it was determined that using the thermal properties of the AEDC 17-4 stainless steel in conjunction with the probe measured temperature gave the best agreement with computed laminar heat flux. These properties were then used to reduce the data for turbulent flows. Based on the this procedure, it was concluded in Hollis and Collier [1] that the uncertainty in heat-transfer measurements was of the order of $\pm$10–20%.

Because the conditions in the tunnel were changing with time, it was deemed that the quantity $StRe_{\infty D}^{0.5}$, which is equal to

$$StRe_{\infty D}^{0.5} = \left(\frac{q}{\rho U \Delta H}\right) Re_{\infty D}^{0.5}, \qquad \Delta H = C_p(T_0 - T_w) \tag{2}$$

where St and Re are the Stanton and Reynolds numbers, respectively, and T_0 is the stagnation temperature, provides a more accurate measurement of the heat flux. Equation (2) is a special case of the Reynolds analogy for a laminar flat plate where $St_x Re_x^{0.5} =$ constant.

A sample of measurements of q, $StRe^{0.5}$, and T_w is shown in Fig. 2. Note that the measured value of $StRe^{0.5}$ is higher than the constant obtained from the Reynolds analogy. This is because the Reynolds number is based on the diameter of the model. It is to be noted that, when quasisteady calculations are employed, one cannot allow for changes in tunnel and surface conditions with time, and average values over the run duration have to be assumed.

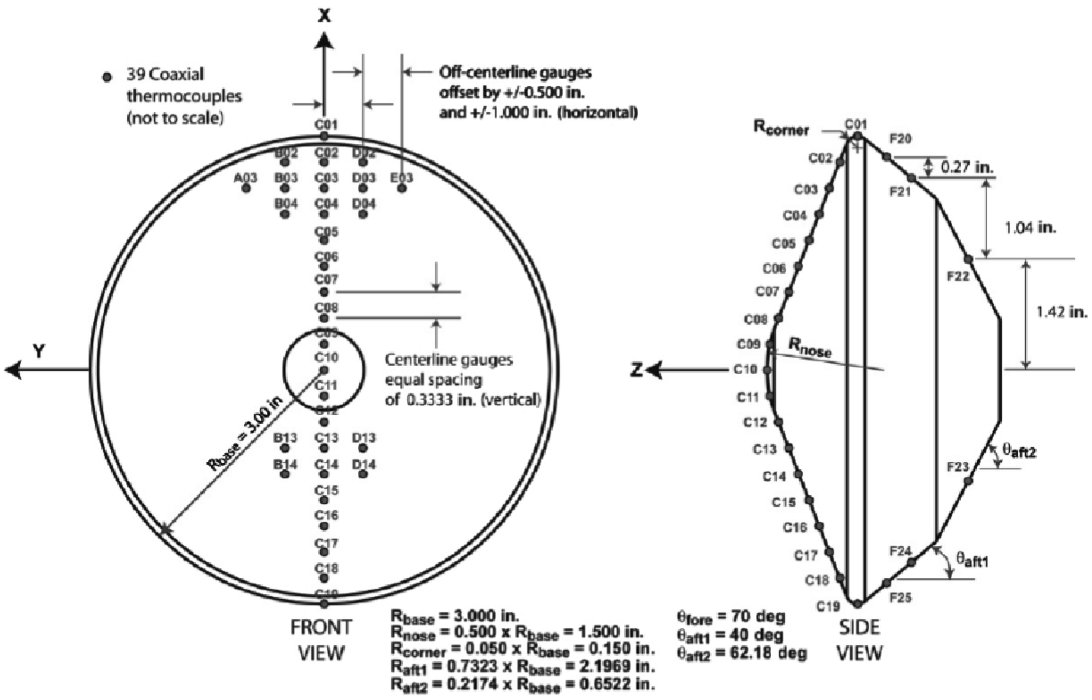

Fig. 1 Model dimensions with thermocouple locations.

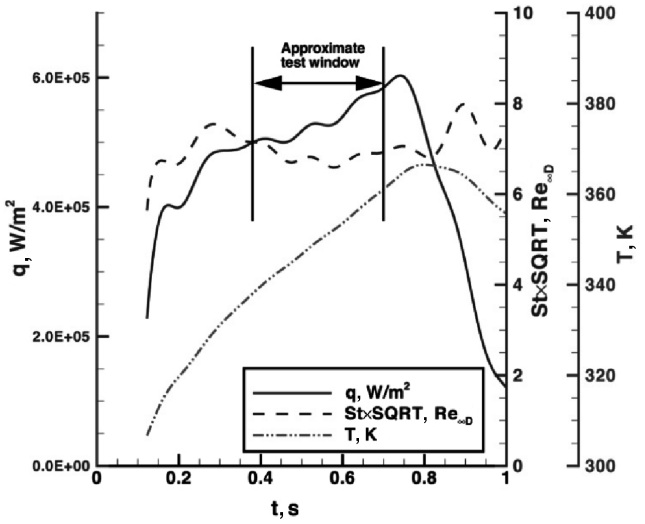

Fig. 2 Mach 8 run AEDC Tunnel 9 gauge temperature and heat-transfer parameters.

D. Computational Method

The LAUARA code is a three-dimensional finite volume solver that includes perfect gas, equilibrium, and nonequilibrium chemistry models. Only perfect gas calculations were carried out in this investigation. Time integration to steady state is accomplished by either point Jacobi or line relaxation. Roe-averaging with Harten's entropy fix and Yee's symmetric variation diminishing limiter is used for inviscid fluxes, and a second-order central difference scheme is employed for the viscous fluxes.

E. Grid

The grid employed is identical to that used in Hollis and Collier [1]. It consists of 14 blocks and employs over 2.2 million grid points. Based on the work of Hollis and Collier [1], resulting solutions are grid independent.

III. Results and Discussion

The AEDC test was conducted in a continuous-pitch mode with the result that the heating data were obtained over the entire angle of attack range of each run. However, because the current trim angle for the MSL is 16 deg, results were computed for this angle only. Heating rates for a specific angle of attack were generated from the data set by averaging over a time interval encompassing ± 0.5 deg from the nominal value.

All calculations presented assume fully developed turbulent flows over the entire body even when experiment indicates that the flow is transitional. This is because the goal of this effort is to determine how well existing turbulence models predict turbulent heating at high Mach and Reynolds numbers. In spite of the fact that the actual measured wall temperatures were not uniform, all calculations were carried out assuming a wall temperature equal to that of the nose gage, which is about 337 K. This will contribute to some discrepancy between the measured and calculated heat-transfer rates. Its extent

Table 1 MSL entry vehicle geometry

Run	Re_∞, 1/ft	M_∞	P_∞, Pa	T_∞, K	ρ_∞, kg/m^3	u_∞, m/s
3025	1.89E + 07	10.3	2126.7	49.6	0.1444	1485.1
3026	1.83E + 07	10.3	2159.0	51.1	0.1423	1506.1
3048	4.96E + 07	8.0	11918.6	69.3	0.5792	1350.9
3051	2.17E + 07	7.8	6399.0	78.4	0.2753	1401.5
3052	2.19E + 07	7.8	6364.5	77.7	0.2765	1395.4
3053	3.02E + 07	7.8	8186.0	73.8	0.3742	1356.6

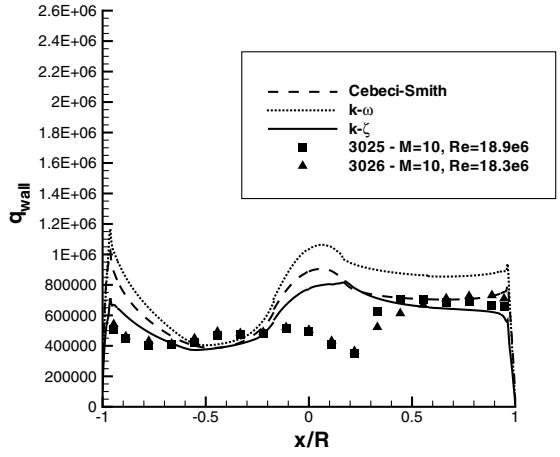

Fig. 3 Comparison of heat flux for $M = 10$ and $Re = 18.5 \times 10^6$/ft.

cannot be determined without a time accurate calculation. All cases considered are summarized in Table 1.

All comparisons are along the centerline of the model for the range of $-1.0 \leq x/R \geq 1.0$, where x is the distance along the center line and R is the radius of the model. Positive values of x/R indicate the lee side, and negative values the wind side. Figure 3 compares computed and measured heat flux for $Re = 18.5 \times 10^6$/ft and $M = 10$. The flow is transitional in this case but is turbulent on the lee side. It is seen from the figure that the CS is in good agreement with the turbulent heat flux on the lee side. The k–ζ is slightly underpredicting the heat flux, whereas the k–ω is overpredicting the heat flux. It appeared to us that the k–ω model was correctly implemented in LAURA. However, the k–ω model has the tendency to overpredict the turbulent eddy viscosity, and this can lead to increased heating rates. Another observation pertains to the region around $x/R = -1.0$. The computed spike in the heat flux is a result of the fact that not enough grid resolution is available around the corners. This spike at the corners is less evident in the k–ζ case. As will be seen later, this behavior is repeated in the remaining calculations.

The aforementioned case represents the highest Reynolds number for which data are available at $M = 10$. The remaining cases are for $M = 8$. Figure 4 compares computed and measured heat flux for $Re = 21.9 \times 10^6$/ft. Here, the CS and k–ζ show good agreement with the experiment, whereas the k–ω predicts higher heating rates on the lee side. The k–ζ results on the lee side lie between both of the experimental sets of data, whereas the CS agrees better with the higher of the two data sets. However, the k–ζ tends to underpredict the stagnation point heating for this case. This trend is seen in the later cases as well. Figure 5 compares calculated and measured heat flux

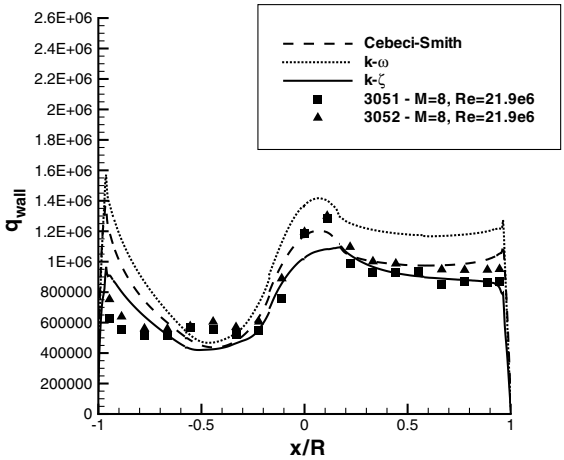

Fig. 4 Comparison of heat flux for $M = 8$ and $Re = 21.9 \times 10^6$/ft.

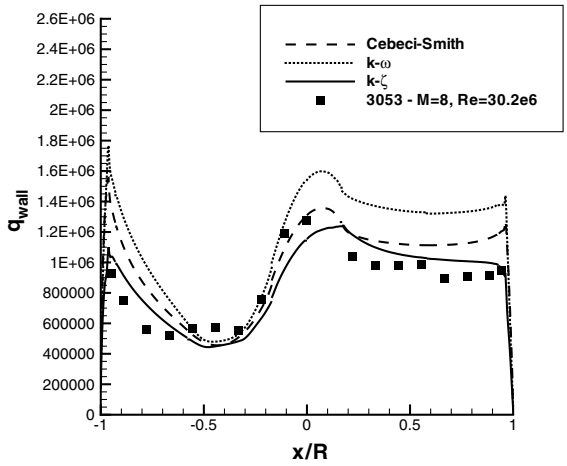

Fig. 5 Comparison of heat flux for $M = 8$ and $Re = 30.2 \times 10^6/\text{ft}$.

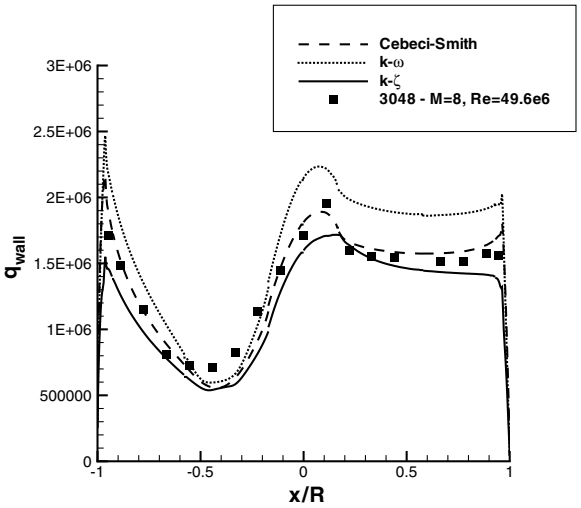

Fig. 6 Comparison of heat flux for $M = 8$ and $Re = 49.6 \times 10^6/\text{ft}$.

for $Re = 30.2 \times 10^6/\text{ft}$ and $M = 8$. It is seen that all three models overpredict the turbulent heating on the lee side. It is not clear whether this is a result of data reduction or wall temperature. However, for this case, the k–ζ is closest to the experimental data on the lee side while still underpredicting the stagnation point heating. Figure 6 compares heat flux for $Re = 49.6 \times 10^6/\text{ft}$ and $M = 8$. The CS slightly overpredicts the lee side heating, whereas the k–ζ slightly underpredicts the lee side heating. Again, the k–ζ underpredicts the stagnation point heating and the k–ω overpredicts the heating at the stagnation point and on the lee side.

IV. Conclusions

Calculations are presented to determine the aerodynamic heating to the forebody of the MSL entry vehicle for some of the tests carried out at Mach 8 and 10 and a range of Reynolds numbers in the AEDC Tunnel 9, assuming quasisteady conditions. In spite of the uncertainties involved in reducing the data, it is concluded that existing turbulence models are capable of predicting heating rates for attached flows. For such flows, algebraic models perform as well as more elaborate models.

Entry into the Martian atmosphere will encounter laminar/transitional and turbulent flows. Thus, there is a need to incorporate transitional/turbulence models into existing production codes, to conduct computations and tests for complete configurations, and to employ more accurate methods for reducing experimental data. This is the only way we can gain enough confidence in the prediction of computational approaches. This will, in turn, lead to more efficient vehicle designs.

Acknowledgment

This work was supported in part by a National Institute of Aerospace Graduate Research Grant.

References

[1] Hollis, B. R., and Collier, A. S., "Turbulent Aeroheating Testing of Mars Science Laboratory Entry Vehicle in Perfect-Gas Nitrogen," AIAA Paper 2007-1208, Jan. 2007.

[2] Marren, D., and Lafferty, J., "The AEDC Hypervelocity Wind Tunnel 9," *Advanced Hypersonic Test Facilities, Progress in Aeronautics and Astronautics*, Vol. 198, AIAA, Reston, VA, 2002, pp. 467–477.

[3] Gnoffo, P. A., "An Upwind-Biased, Point-Implicit Relaxation Algorithm for Viscous, Compressible Perfect-Gas Flows," NASA TP-2953, Feb. 1990.

[4] Cheatwood, F. M., and Gnoffo, P. A., "User's Manual for the Langley Aerothermodynamics Upwind Relaxation Algorithm (LAURA)," NASA TM-4674, April 1996.

[5] Cebeci, T., and Smith, A. M. O., *Analysis of Turbulent Boundary Layers*," Series in Applied Mathematics and Mechanics, Vol. 25, Academic Press, Orlando, FL, 1974.

[6] Wilcox, D. C., *Turbulence Modeling for CFD*, 2nd ed., DCW Industries, Inc., La Canada, CA, 1998.

[7] Hassan, H. A., and Robinson, D. F., "Further Development of the k–ζ (Enstrophy) Turbulence Closure Model," *AIAA Journal*, Vol. 36, No. 10, 1998, pp. 1825–1833.